UCRL-PROC-207450

LAWRENCE
LIVERMORE
NATIONAL
LABORATORY

Improved Energy Coupling into the Gain Region of the Ni-like Pd Transient Collisional X-ray Laser

R. F. Smith, J. Dunn, J. Nilsen, S. Moon, R. Keenan, R. Shepherd, R. Booth, J. R. Hunter, J. Filevich, J. J. Rocca, M. C. Marconi, V. N. Shlyaptsev

October 25, 2004

9th International X-ray Laser Conference
Beijing, China
May 24, 2004 through May 28, 2004

Improved Energy Coupling into the Gain Region of the Ni-like Pd Transient Collisional X-ray Laser

R.F. Smith, J. Dunn, J. Nilsen, S. Moon, R. Keenan, R. Shepherd, R. Booth, J. R. Hunter

Lawrence Livermore National Laboratory, Livermore, CA 94551

J. Filevich, J.J. Rocca, M.C. Marconi

NSF ERC for Extreme Ultraviolet Science and Technology and Department of Electrical and Computer Engineering, Colorado State University, Fort Collins, Colorado 80523

V.N. Shlyaptsev

University of California Davis-Livermore, Livermore, CA 94551

Abstract. We combine near-field imaging with the recently developed technique of picosecond x-ray laser interferometry to probe the plasma conditions in which the Ni-like Pd transient collisional x-ray laser is generated and propagates. We observe a strong dependence of the laser pump parameters on the effective laser-gain medium coupling. The most effective coupling of laser pump energy occurs when the duration of the main heating pulse is comparable to the gain lifetime (~10ps for mid-Z Ni-like schemes). This can increase the output intensity by more than an order of magnitude relative to the case were the same pumping energy is delivered within a shorter heating pulse duration (< 3ps). The higher intensity heating pulses are observed to be absorbed at higher electron densities and in regions were steep density gradients limit the effective length of the gain medium.

1. Introduction

Lasing at EUV wavelengths is typically generated through single pass amplification along an extended laser-produced plasma column. One of the goals driving x-ray laser research is the prospect of obtaining saturated lasing within the wavelength range between the K absorption edges of carbon (4.37 nm) and oxygen (2.33 nm), the "water window" where carbon-containing biological objects absorb radiation efficiently but water is relatively transparent. This would facilitate powerful new diagnostic techniques of high contrast sub-micron imaging of live biological samples [1]. In recent years saturated lasing has been demonstrated on a number of wavelengths in the 5.7 to 60.8nm range [2]. Currently the most efficient lasing at short wavelengths (λ < 15nm) has been observed on the $4d^1S_0 \rightarrow 4p^1P_1$ atomic transition in the closed shell Ni-like ion species. The wavelength output for this transition scales as ~Z^3, where Z is the atomic number of the material. For higher atomic numbers greater ionization, and hence greater input energy is required to achieve the Ni-like ion state. As a result, saturated operation at wavelengths below ~10nm have only been demonstrated on large laser facilities.

In all laser pumped schemes a variation of the prepulse pumping technique is employed whereby a low intensity long pulse preforms a plasma, which is allowed to expand and cool before being heated by a high intensity main pulse. In the transient collisional excitation (TCE) scheme [3] this main heating pulse is temporally compressed by chirped pulse amplification (CPA) techniques down to picosecond durations. The CPA pulse rapidly heats the plasma generating high gain coefficients and saturated x-ray laser output over a few picoseconds duration [4]. In experiments reported on high power laser drivers the pulse duration of the CPA pulse is in the range of 0.5 → 3ps [5, 6, 7]. It has been felt that by maximizing the intensity of the main heating pulse the local gain coefficient will also be maximized. Under these conditions the lowest saturated wavelength currently demonstrated is 7.3 nm for Ni-like Sm [5]. Within this paper we show that high intensity heating of the x-ray laser gain medium can be detrimental to the effective gain-length product. It is observed that by matching the duration of the main pumping pulse to the duration of the gain optimizes the coupling efficiency and increases the x-ray laser output by an order of magnitude. This more effective use of the laser pump energy offers a more efficient route to lower wavelength operation. High intensity heating pulses are shown to deposit their energy at high electron densities were increased levels of refraction limit the gain-length product.

2. Experiment

The Ni-like Pd x-ray laser at 14.68 nm is generated using two laser beams at 1054 nm wavelength from the COMET table-top laser facility at LLNL [8]. Saturated x-ray lasing output of ~10 μJ is achieved with an optical pumping combination of a 600 ps long pulse (1.5 J, $\sim 1 \times 10^{11}$ W cm^{-2}) and a temporally compressed (0.5 → 27ps) main heating pulse (4 J, $5 \rightarrow 0.1 \times 10^{14}$ W cm^{-2}). A 1.6 cm x 140μm line focus employed in a traveling wave geometry is used to irradiate a 1.25 cm long polished Pd slab target [8]. A series of shots were taken in which the output plane of the x-ray laser plasma column was imaged by a 11.75cm focal length spherical multilayer mirror and relayed onto a charged coupled device (CCD) camera with a magnification of ~22 giving a two-dimensional intensity map of the x-ray laser 'footprint' as a function of distance away from the target surface. The peak-to-peak separation between the long and short pulse (Δt) was varied in intervals from 0 → 1ns, the CPA pulse duration was varied from 500fs → 27ps and the resulting x-ray laser output intensity map was recorded.

3. Results

By integrating over the area of the footprint and taking into account the measured pulse durations [4] we can determine the relative output intensity of the x-ray laser as a function of laser pump parameters (Fig. 1). The highest output is observed for the main heating pulse durations of 6.7 and 13.4ps and for a Δt of ~700ps. Under these pumping conditions previous measurements have determined the x-ray lasing transition to be saturated [8]. The outputs for the shorter duration CPA pulses (1.7ps and 0.5ps), however, are more than an order of magnitude less than for the 13ps case and are therefore considered to be unsaturated. As the CPA pulse duration is increased to ~27ps the x-ray laser output intensity falls off from the peak value. For a given heating pulse duration there is a strong dependence on the x-ray laser output as a function of Δt.

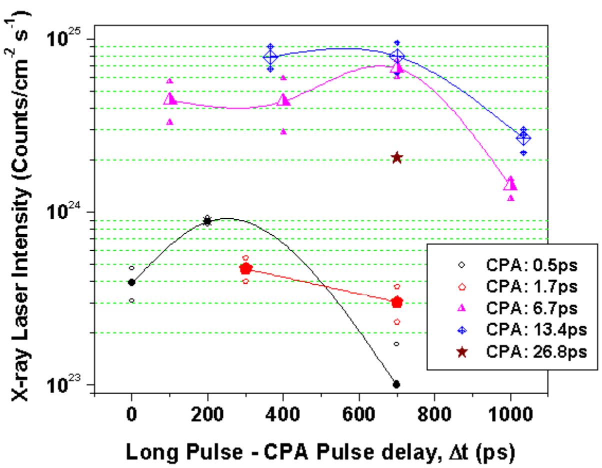

Fig 1. X-ray laser output intensity as a function as laser pumping parameters. The standard operating conditions for the x-ray laser on the COMET laser facility is for a CPA pulse duration of 13.4ps with a Long pulse – Short pulse delay, Dt, of 700ps. The duration of the x-ray laser pulse as reported in Ref [4] is shown in brackets when measured for a Dt of 700ps.

Simulations with the 1D Lasnex code [9] shown in figure 2 show the calculated gain profile for the $4d^1S_0 \rightarrow 4p^1P_1$ gain transition as a function of distance away from the target surface (x-axis) and time relative to the peak of the CPA heating pulse. The duration of the gain is ~10 ps irrespective of the duration of the heating pulse. This is supported by recent measurements in which the output pulse durations which only change by a factor of two (~ 4 → 8ps) when the duration of the main heating pulse is changed by a factor of 55 (0.5 → 27.8ps) [4]. For short CPA pulse durations (< 3ps) the plasma is heated very rapidly, the energy is deposited at higher densities and in regions of larger density gradients than for longer CPA heating pulses (see below). We can see from the contour plot in Fig. 2 (a) the peak of the gain in the plasma heated by the 0.5ps heating pulse occurs after the laser irradiation is switched off. The higher short pulse intensity is not coupled efficiently and as a result the effective gain coefficient is less. It is possible to drive the shorter heating pulsed driven x-ray laser into saturation but it requires higher intensities to do so [5, 6, 7]. Pumping pulse durations < 3ps are typically used on large laser facilities. The shorter duration heating pulses exhibit slightly enhanced output for reduced values of Δt. This is consistent with ref [3] which showed optimized Δt of ~150ps for Ni-like Sm when pumped with a 1ps CPA pulse. This is not a result of more effective beam propagation but is expected to be representative of the higher local gain coefficient for early Δt due to the presence of higher temperatures and densities. Refraction is expected to limit the extent to which this high gain region is sampled. For the lower intensity longer CPA pulses shown in Fig 2(b) (6.7ps and 13.4ps) the heating occurs over the same time scale and during the same time period as the gain duration and the energy is coupled more effectively into the gain region, resulting in enhanced output. For the 27ps (Fig. 2(c)) case the gain has dissipated before most of the energy has even been delivered on target. Therefore the coupling effectivity is poor and the x-ray laser output intensity drops. For all the CPA pulse durations there are variations in the output with Δt. It is expected that at later times (Δt: 700ps) the density gradients have relaxed sufficiently to optimise the beam guiding of the x-ray laser photons. As a result the energy output of the x-ray laser is maximised.

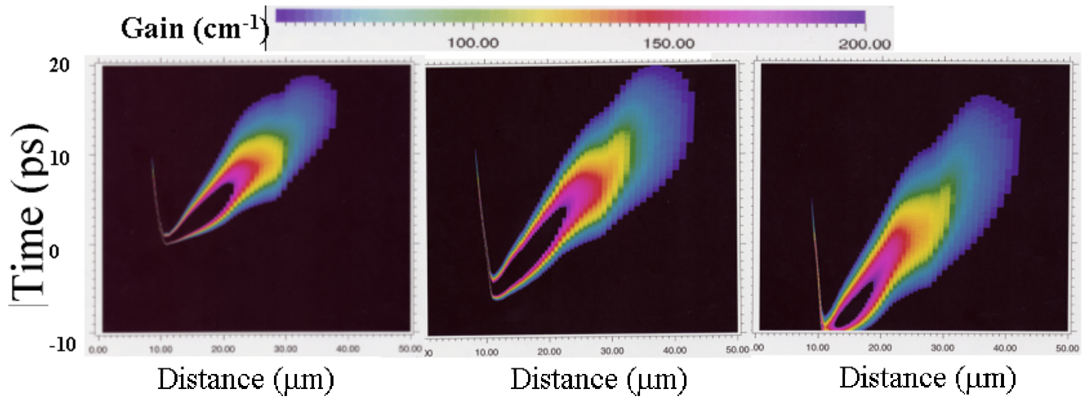

Fig 2. 1D Lasnex simulations show that the gain profile within the x-ray laser medium is centered in time around the optical pumping of a 10ps+/-3ps heating pulse. For CPA pulse durations < 3ps the peak of the gain occurs after the optical heating pulse is turned off. For the 26.8ps heating pulse the gain occurs at the leading edge of the pulse and is extinguished before the peak of the energy is delivered. The color table for gain saturates in the centre of the contours at values of 200cm^{-1}.

Previous work has shown that the combination of the Ni-like Pd transient collisional x-ray laser with a diffraction grating interferometer offers unique diagnostic capabilities in accurately measuring two-dimensional electron density maps of laser-produced plasmas [8]. The picosecond timescale and short wavelength output mitigate effects due to refraction, absorption and motion blurring making this technique appropriate for accurately diagnosing the long millimeter scale plasmas, which are characteristic of the x-ray laser gain medium. Simulations of the x-ray laser medium have shown [7] that the electron density profile setup by the long pulse remains relatively unperturbed (± 5%) during the interaction of the main CPA heating pulse and the time period over which gain and x-ray laser propagation takes place. Therefore, by interferometrically measuring the 2D electron density profile at a chosen delay after the peak of the 600ps long pulse, we are observing the density conditions in which the x-ray laser gain is generated and in which the x-ray laser pulse subsequently propagates.

Within one arm of the interferometer a plasma was formed from a Pd target using the same irradiation conditions as those implemented for the 600ps long pulse used to generate the x-ray laser. A 3.2mm x 140μm line focus was generated on the plane of a 2mm long polished Pd target via the combination of a cylindrical lens and off-axis parabola. The energy delivered in the line focus was 300mJ which gives an on-target intensity of ~1×10^{11} W/cm^2. The x-ray laser probe beam travels longitudinally through the resultant Pd plasma. The output plane of the plasma is imaged via a 25cm focal length Mo/Si multilayer optic and relayed to a 13μm pixel CCD camera ~5.5m away giving an average magnification of ~22. The number of fringe shifts, N_{fringe}, is related to the electron density n_e by [10], $N_{fringe} \cong (n_e L)/(2n_{crit} l)$, where n_{crit} is the critical density for the probe wavelength l and L is the plasma length. For the 2mm target used, one fringe shift is equivalent to an electron density of ~7.6×10^{19} cm^{-3}. Using this technique the 2D electron density profile was measured at different delays relative to the peak of the 600ps plasma forming beam. Within the x-ray laser context these times can be understood as different long pulse → CPA pulse delays (Δt). The average ionisation for the Pd plasma from Δt = 0 → 1ns was calculated to be between 14 to 16. Under these conditions the contribution for the bound electrons to the refractive index within the Pd plasma is expected to be small.

By overlaying the near field images with the density maps obtained through interferometry we can determine the density at which the x-ray laser footprint exits the plasma column. As the x-ray laser is generated in a traveling wave geometry the electron density through which the x-ray propagates is effectively frozen over the ~ 4 picosecond pulse duration. The extracted density profiles, therefore, represent a good picture of the conditions within the frame of the propagating x-ray laser. Simulations predict that the region which contributes most effectively to the x-ray laser amplification lies at an electron density of $\sim 1\times10^{20}$ cm^{-3} [10]. Shown in figures 3(a) and (b) are the combined density and intensity maps at the output of the x-ray laser gain medium for a Δt of 0.7ns and a CPA pulse duration of 0.5 and 6.7ns, respectively. The 500fs heating pulse produces an x-ray laser output centered at $\sim 5\times10^{19}$ cm^{-3} while for the same density conditions the low intensity 6.7ps heating pulse generates an x-ray laser output centered at 1×10^{20} $cm^{-3.}$ The angle of refraction may be approximated to be inversely proportional to the density scale length of the plasma [11]. The extent of this deflection gives an indication of how long the x-ray laser photons remain within the gain region, which ultimately determines the extent of amplification. This suggests that the region contributing most the gain for the short CPA case is at a higher density were larger density gradients exist than for the 6.7ps CPA case. This is consistent with Lasnex simulations, which predict that the shorter CPA pulse durations deposit their energy preferentially within higher density regions. For the 6.7 ps heating pulse the energy is deposited in a region with more relaxed density gradients yielding reduced refraction and as a consequence the x-ray laser photons spend a long time within the gain region and experience greater amplification. At this image plane the x-ray laser has traversed through the 12.5 mm long amplifying medium with very small deflection. It is apparent from these images that the dimensions of the x-ray laser output are influenced greatly by the laser parameters. We note that as the x-ray laser becomes more saturated the footprint becomes more concentrated in space, which is a result of the localized region of high gain dominating the amplification process.

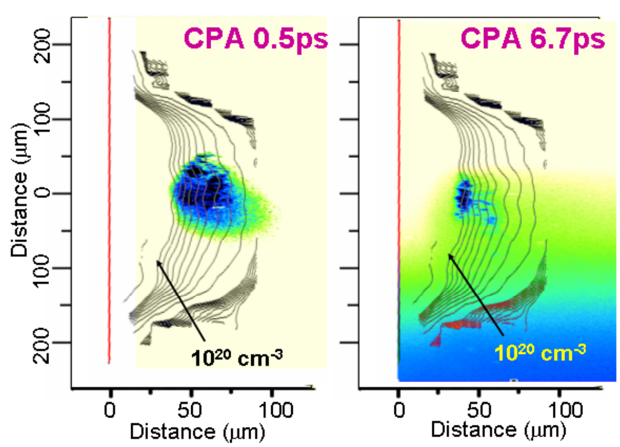

Fig 3. The footprint of x-ray laser is overlaid on interferometrically determined electron density maps. The CPA pulse duration is 0.5ps and 6.7ps for figure (a) and (b), respectively. In both cases the value for Dt was 0.7ns. The color scales have been optimized for each particular image in order to enhance detail. The relative outputs are shown in figure 1. The extracted electron density contour map is shown in a logarithmic scale with each line connecting regions of equal density. The 10^{20} cm^{-3}

contour is highlighted, as this is the density at which the most effective gain contribution is predicted to originate from.

We have also observed from the near field images that the beam profile is more structured for the shorter duration CPA pulses. These observations are consistent with recent measurements that show that the spatial coherence of the x-ray laser also increases for longer duration CPA drivers [12]. As the near field monitor is time integrated there will be some smoothing effect from the longer pulse durations. However as the x-ray laser pulse duration is largely insensitive to the main heating pulse width this does not explain the observations. The reduced structure at longer heating pulse durations may be due to smoothing effects by the optical beam. In the 500fs case the drive beam is turned off many picosecond before the x-ray laser is generated. Spatial inhomogeneities in the intensity profile are imprinted instantaneously [13] and without any further energy being deposited into the plasma, non-uniformities in the gain profile may result. For longer CPA pulse drivers imprinting also occurs at the leading edge of the pulse but at lower intensities. In addition, as energy is being deposited for many picoseconds, smoothing from continued coupling of the drive laser is likely to aid dissipation of the initial imprinted non-uniformities.

We have conducted a series of experiments studying the effect of varying the laser pump parameters on the x-ray laser performance which has showed that by matching the duration of the CPA pulse with the gain duration (~10 ps) an enhancement in the x-ray laser output intensity by more than an order of magnitude was achieved over the short CPA pulse case (< 2 ps). By keeping the density conditions constant, we infer from the increased levels of refraction that short CPA pulses deposit their energy at densities higher than for the longer CPA pulses (as predicted by simulations).

The support of Al Osterheld and Andy Hazi is greatly appreciated. The authors are pleased to acknowledge the technical contributions from Carl Bruns and Al Ellis. This work was performed under the auspices of the U.S. Dept. of Energy by the University of California Lawrence Livermore National Laboratory, through the Institute for Laser Science and Applications, under Contract No. W-7405-Eng-48 and by US Department of Energy Grant No. DE-FG03-98DP00208. This research was sponsored by the National Nuclear Security Administration under the Stewardship Science Academic Alliances program through DOE Research Grant # DE-FG03-02NA00062. The CSU researchers also gratefully acknowledge the partial support of the NSF ERC Center for Extreme Ultraviolet Science and Technology, award number EEC-0310717 and the W.M. Keck Foundation.

References

[1] Solem J C and Baldwin G C, “Microholography of living organisms”, Science **218**, 229 (1982).

[2] Daido H, “Review of soft x-ray laser researches and developments.” , Reports on Progress in Physics, vol.65, no.10, pp.1513-76, (2002).

[3] Shlyaptsev V N, Nickles P V, Schlegel T, Kalashnikov M P, Osterheld A L, “Table-top X-ray laser pumped with subnanosecond and picosecond pulses”, Proceedings of the SPIE - The International Society for Optical Engineering, (Ultrashort Wavelength Lasers II, San Diego, CA, USA, 12-13 July 1993.) **2012**, pp.111-18 (1993).

[4] Dunn J, Smith R.F., Nilsen J., Shepherd R., Shlyaptsev V.N., Booth R., Hunter J.R., "Characterization of a Picosecond Laser-Pumped X-ray Laser", these proceedings.

[5] King R E, Pert G J, McCabe S P, Simms P A, MacPhee A G, Lewis C L S, Keenan R, O'Rourke R M N, Tallents G J, Pestehe S J, Strati F, Neely D, Allott R, "Saturated x-ray lasers at 196 and 73 Å pumped by a picosecond traveling-wave excitation", Phys. Rev. A **64**, 053810 (2001).

[6] Klisnick A, Zeitoun P, Ros D, Carillon A, Fourcade P, Hubert S, Jamelot G, Lewis C L S, MacPhee A G, Rourcke R M N, Keenan R, Nickles P V, Janulewicz K, Kalashnikov M, Warwick J, Chanteloup J-C, Migus A, Salmon E, Sauteret C, Zou J P**, "**Transient pumping of a Ni-like Ag x-ray laser with a subpicosecond pump pulse in a traveling-wave irradiation geometry", J. Opt. Soc. Am. B **17**, *pp.1093-7* (2000).

[7] Tang H, Daido H, Kishimoto M, Sukegawa K, Renzhong Tai, Mosesson S, Tanaka M, Peixiang Lu, Kawachi T, Nagashima K, Nagai K, Norimatsu T, Murai K, Takenaka H, Kato Y, Mima K, Nishihara K, "Spatial coherence measurement of 13.9 nm Ni-like Ag soft X-ray laser pumped by a 1.5 ps, 20 J laser", Japanese Journal of Applied Physics Part 1-Regular Papers Short Notes & Review Papers **42**, no.2A, pp.443-8. (2003).

[8] Dunn J, Li Y, Osterheld A L, Nilsen J, Hunter J R, Shlyaptsev V N, "Gain saturation regime for laser-driven tabletop, transient Ni-like ion X-ray lasers", Phys. Rev. Lett. **84**, 4834 (2000).

[9] Zimmerman G B and Kruer W L, Comments on Plasma Physics for Controlled Thermonuclear Fusion **2**, 51-61 (1975).

[10] Smith R F, Benredjem D, Moller C, Kuba J, Klisnick A, Pert G J, Upcraft L, King R, Gauthier J-C, Drska L, "Modeling of the transient Ni-like Ag X-ray laser", SPIE-Int. Soc. Opt. Eng. Proceedings of Spie - the International Society for Optical Engineering **4505**, pp.107-15 (2001).

[11] Smith R F, Dunn J, Nilsen J, Hunter J R, Shlyaptsev V N, Rocca J J, Filevich J, Marconi M C, "Refraction Effects on X-ray and UV Interferometric Probing of Laser Produced Plasmas", JOSA B **20**, Issue 1, p. 254 (2003).

[12] We measured the spatial coherence of the x-ray laser output with a Young's double slit experiment. The distance between the slits was systematically varied and backlit by the x-ray laser generated with different CPA pulse durations. It was observed that the spatial coherence improved as a function of increasing CPA pulse duration. This data is unpublished.

[13] Glendinning S G, Weber S V, Bell P, DaSilva L B, Dixit S N, Henesian M A, Kania D R, Kilkenny J D, Powell H T, Wallace R J, Wegner P J, Knauer J P, Verdon C P. "Laser-driven planar Rayleigh-Taylor instability experiments" Phys. Rev. Lett. **69**, 8, pp.1201-4, (1992).